Template Matching and Particle Filtering for Structural Identification of High- and Low-Frequency Vibration

Chapter · July 2022

DOI: 10.1007/978-3-031-04098-6_5


Nicholas A. Valente
University of Massachusetts Lowell


Celso do Cabo
Worcester Polytechnic Institute


Zhu Mao
Worcester Polytechnic Institute

This is a preprint version. The published version is available at:
https://doi.org/10.1007/978-3-031-04098-6_5

Template Matching and Particle Filtering for Structural Identification of High and Low Frequency Vibration

Nicholas A. Valente[1], Celso T. do Cabo[1, 2], Zhu Mao[1, 2†], Christopher Niezrecki[1]

1. Department of Mechanical Engineering, University of Massachusetts Lowell, Lowell, MA 01854, USA

2. Department of Mechanical Engineering, Worcester Polytechnic Institute, Worcester, MA 01609, USA

ABSTRACT

Digital image correlation (DIC) has been widely accepted in the vibration community for extracting strain and displacement using noncontact optical techniques. Due to the nature of DIC, the preparation of a test structure with an applied pattern is important for obtaining accurate results. Investigation into pattern-less optical methods would be beneficial and it would be ideal if a test structure no longer needed pre-treatment prior to optical testing. Recently in the literature, Phase Based Motion Magnification (PMM) has been utilized to exaggerate subtle motion for structural identification. In this work, template matching is used to correlate a template facet over a series of magnified images. Following the determination of a template facet, virtual red, green and blue (RGB) targets are placed along the principal direction of displacement. Particles are then randomly generated and used to find the RGB coded targets and clustered to obtain sub-pixel displacements that can be used for frequency extraction of magnified data. Application of the template match particle filter (TMPF) approach will further enhance non-contact sensing, in addition to providing a more efficient way of processing optical data. This method is implemented to experimentally characterize parameters of two structures (i.e. a cantilever beam and bridge) having both high and low frequencies.

Keywords: Phase Based Motion Magnification, Digital Image Correlation, Particle Filter, K-Means Clustering, Frequency Extraction

INTRODUCTION

Non-contact sensing is a broad research topic that aims to gather data remotely rather than with physical sensors. Optical techniques are adopted for structural dynamic evaluation due to the laborious task of instrumenting a structure. Larger structures typically oscillate at a lower frequency and can make it difficult to extract structural dynamic parameters. To combat this, adoption of phase-based motion magnification (PMM) has proven to be successful in amplifying subtle motion [1]. This approach has been applied to extract structural dynamic behavior ranging from wind-turbine blades, bridges and other complex architecture [2-6]. In recent years, there has been improvements in the motion magnification technique using machine learning and image enhancement approaches [7, 8]. This augmentation of the phase-based algorithm can aid in extracting structural dynamic parameters such as resonant frequencies and operating shapes more easily [9-16]. Recently, adoption of template matching and particle filters have been used to evaluate complex dynamics [17-20]. The implementation of said approaches have created a more autonomous way of analyzing dynamics. In this work, a combination of both template matching

† *Corresponding author:*
E-mail address: zmao2@wpi.edu

and particle filtering (TMPF) will aid characterizing the motion of both a cantilever beam and full-scale bridge structure.

BACKGROUND

Template matching has been a computer vision tool that has permitted region of interest tracking over a sequence of images. The use of normalized cross-correlation between sequential frames is typically used for optical flow processes such as DIC. A template or facet of pixels, I_1, is selected within a pre-determined window, H, over a n number of frames. The pre-determined template is compared to the sequential video frame, I_2 displaced in the coordinate plane where u and v are displacements in the (x, y) plane. Eq. 1 expresses the relationship between I_1 and I_2, which yields the correlation matrix R [19].

$$R = \frac{\sum_{(u,v)\in H} I_1(u,v) \cdot I_2(x+u, y+v)}{\sqrt{\sum_{(u,v)\in H} I_1^2(u,v) \cdot \sum_{(u,v)\in H} I_2^2(x+u, y+v)}} \tag{1}$$

The correlation matrix contains weights ranging from zero to one that signify low to high correlation between the template and sequential image. The shift in the image template from frame to frame is measured by global pixel displacement. Adoption of the particle filter is used to gain sub-pixel resolution of displacements between frames.

Particle filtering is commonly used in estimation theory with several applications in control systems. Common algorithms such as Kalman filters have shown trialed success in extracting dynamic motion; however, they are limited to linear dynamics and Gaussian noise. The benefit of using the particle filtering algorithm, is its ability to estimate non-linear dynamics in addition to handling non-Gaussian noise. The formulation of the particle filter will not be discussed as it is beyond the scope of this paper, but comments on its application will be highlighted. Particle filters are used to estimate system dynamic or states, which can be used to predict further states as they change in time [21].

$$\begin{Bmatrix} x_n \\ y_n \\ \dot{x}_n \\ \dot{y}_n \end{Bmatrix} = \begin{bmatrix} 1 & 0 & 0 & 0 \\ 0 & 1 & 0 & 0 \\ 0 & 0 & 1 & 0 \\ 0 & 0 & 0 & 1 \end{bmatrix} \begin{Bmatrix} x_{n-1} \\ y_{n-1} \\ \dot{x}_{n-1} \\ \dot{y}_{n-1} \end{Bmatrix} + \begin{Bmatrix} \psi_x \\ \psi_y \\ \dot{\psi}_x \\ \dot{\psi}_y \end{Bmatrix} \tag{2}$$

Within Eq. 2, the location and velocity of the particle filter targets at frame n are represented by (x_n, y_n) and $(\dot{x}_n, \dot{y}_n)$ respectively. The additional terms, $\psi_x, \psi_y, \dot{\psi}_x, \dot{\psi}_y$ are representative of additive noise that is present in the dynamic system. The Euclidean distance, k, between RGB values of the virtual target and the corresponding RGB virtual target vector is expressed as,

$$k = \sqrt{(r - r_i)^2 + (g - g_i)^2 + (b - b_i)^2}, \tag{3}$$

This is a preprint version. The published version is available at:
https://doi.org/10.1007/978-3-031-04098-6_5

where r, g, b are the RGB values of the generated particles in the image and r_i, g_i, b_i are the RGB target values that are to be tracked in the image. Eq. 4 is used to resample the particles and update their location in sequential frames [21].

$$P(Y_n \mid X_{n \mid n-1}) = \frac{1}{\sqrt{2\pi}\sigma} e^{\left(-\frac{k^2}{2\sigma^2}\right)} \tag{4}$$

The likelihood distribution and corresponding standard deviation, σ, relates the Euclidean distance, k and successive dynamic states. As k gets smaller, the particle filter will be tracking the RGB targets in the frame. Due to the number of particles generated, the k-means clustering algorithm is used to localize the target and provide sub-pixel resolution [22]. K-means clustering will aid in taking a cluster of particles and determining an (x, y) coordinate in the image.

ANALYSIS

The objective of PMM is to amplify subtle motion in video for further structural dynamic analysis. For this study, a specific algorithm is created to capture magnified motion using several computer vision approaches. Fig. 1 below, displays the algorithm architecture used to extract magnified time history.

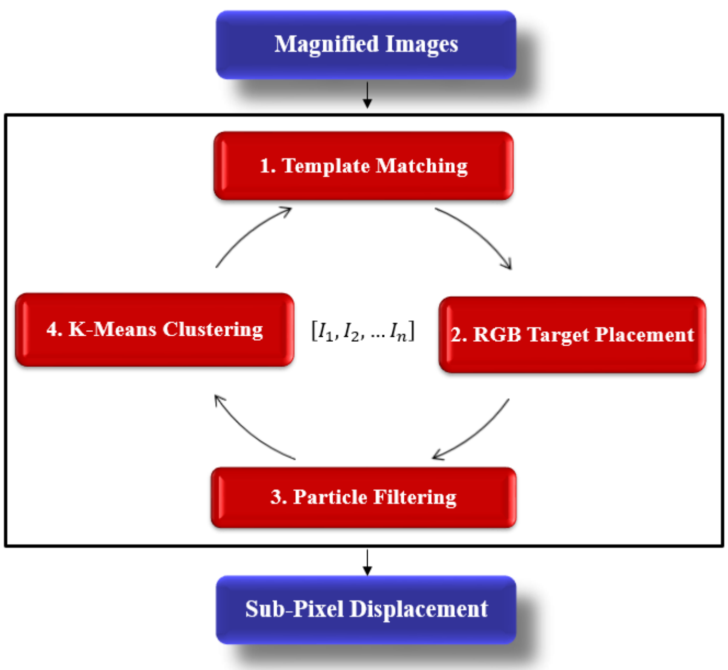

Fig. 1: TMPF algorithm structure for sub-pixel displacement extraction.

Experimental validation is conducted on a cantilever beam and full-scale bridge structure. Both structures are chosen to verify that the proposed algorithm can capture both high and low frequency oscillations. Following the initial capturing of video, a selection of PMM parameters such as: magnification factor and frequency bandwidth are designated for displacement extraction.

This is a preprint version. The published version is available at:
https://doi.org/10.1007/978-3-031-04098-6_5

Beam Experiment

A cantilever beam is used to validate the high-frequency capturing capability of the proposed algorithm. A single 4-megapixel PHOTRON high-speed camera captures data at 2500 (fps). The corresponding calibration factor of approximately 0.4 (mm/pixel). Fig. 2 below displays the experimental setup and frequency response function (FRF) of the cantilever beam.

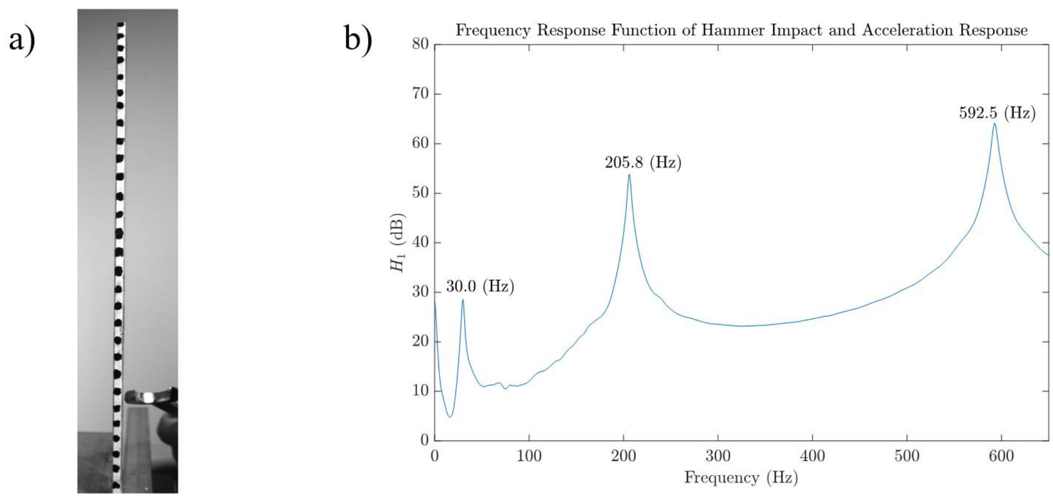

Fig. 2: (a) Image of cantilever beam experiment, (b) FRF of beam excitation and acceleration response up to the third resonant frequency.

Experimental modal analysis (EMA) provides resonant frequencies that are used to compare accelerometer results with TMPF. Following the steps outlined in Fig. 1, TMPF generates 5 elements or templates along the length of the beam that each contain three RGB coded targets, which produces 15 particles in total. The results from the TMPF algorithm are displayed in Fig. 3.

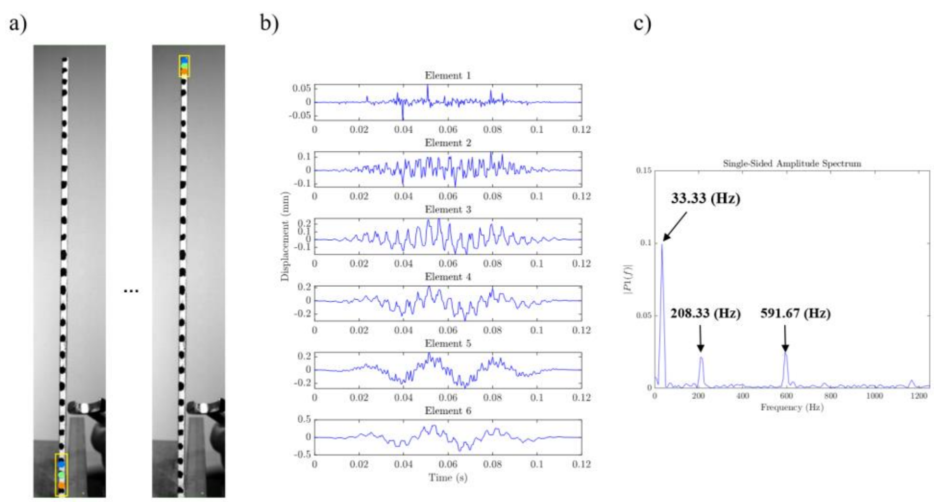

Fig. 3: (a) Template (yellow rectangle) and particle filter RGB coded targets for the first six of ten elements, (b) Mean of extracted displacements using particle filter for the first six of ten templates, (c) Fast Fourier Transform of extracted displacement (Element 6).

This is a preprint version. The published version is available at:
https://doi.org/10.1007/978-3-031-04098-6_5

Given the extraction of time histories for the length of the cantilevered beam, it is also possible to extract operating deflection shapes (ODS) after magnification of resonant frequencies. Table 1 lists the resonant frequencies, magnification band and magnification factor necessary to gain insight into higher order dynamics.

Table 1: Comparative analysis of experimental frequencies, magnification band and factor for each resonant frequency.

Resonant Frequency	**EMA Frequency (Hz)**	**TMPF Frequency (Hz)**	**Magnification Frequency Band** $\omega_l - \omega_h$ **(Hz)**	**Magnification Factor** α
1	30.0	33.3	29.0-35.0	10
2	205.8	208.3	204.0-210.0	15
3	592.5	591.7	590.0 – 595.0	25

Following the magnification of each bending mode, the extracted operating shapes are computed using a peak-picking approach for the length of the beam at the first three resonant frequencies as show in Fig. 4.

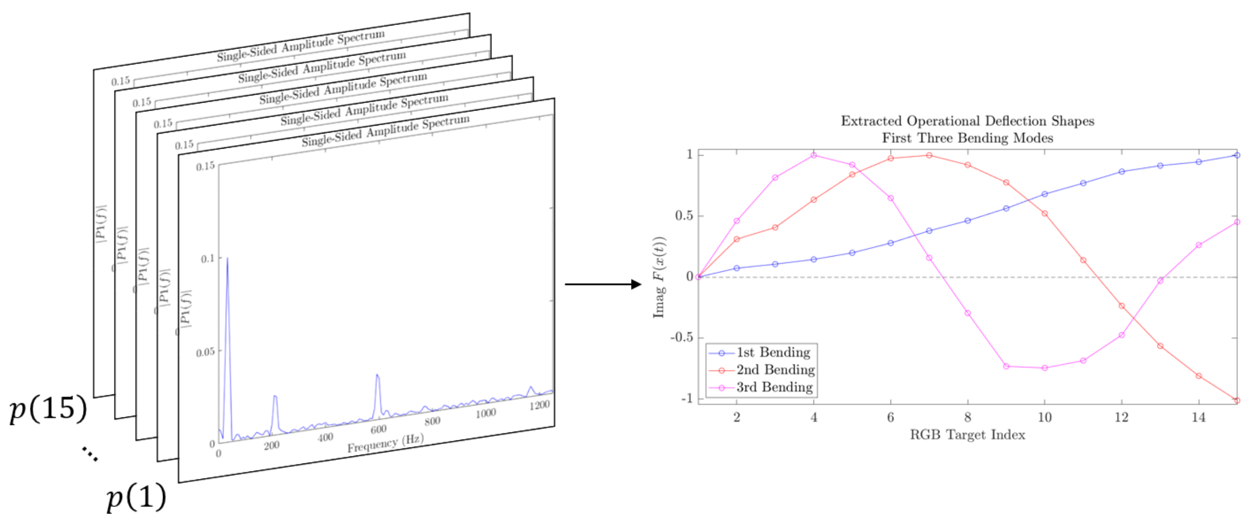

Fig. 4: Peak-picking approach for computation of the first three operating shapes, where $p(1)$ to $p(15)$ represent the fifteen RGB coded targets.

TMPF computes magnified time history in addition to ODS for the cantilever beam. The cross-correlation calculation that is computed using Eq. 1 is necessary to track a region of interest from frame to frame. This is consistent with traditional DIC, where a facet of pixels is chosen to track over a series of images. Hand speckle interferometry makes template matching more simplistic; however, it is not practical on large scale structures due to the pre-treatment necessary for non-destructive evaluation. Following the determination of the reference template using TMPF, the particle filtering and clustering of the RGB coded targets provide sub-pixel resolution of magnified displacement. This will rid the need for pretreatment of a structure so long that a template can be found between sequential frames.

This is a preprint version. The published version is available at:
https://doi.org/10.1007/978-3-031-04098-6_5

Bridge Test

A full-scale, 25 meter span bridge in Maine is used to collect low frequency vibration data via the proposed TMPF approach. This structure does not contain a pre-treatment of DIC's trademark stochastic pattern. Therefore, the computation of dynamics will solely rely on the TMPF approach. A commercial truck is driven over the bridge at 20 (mph) for excitation purposes. As shown in Fig. 5, PMM is implemented to exaggerate the motion of the bridge, such that frequency can be computed using magnified time history.

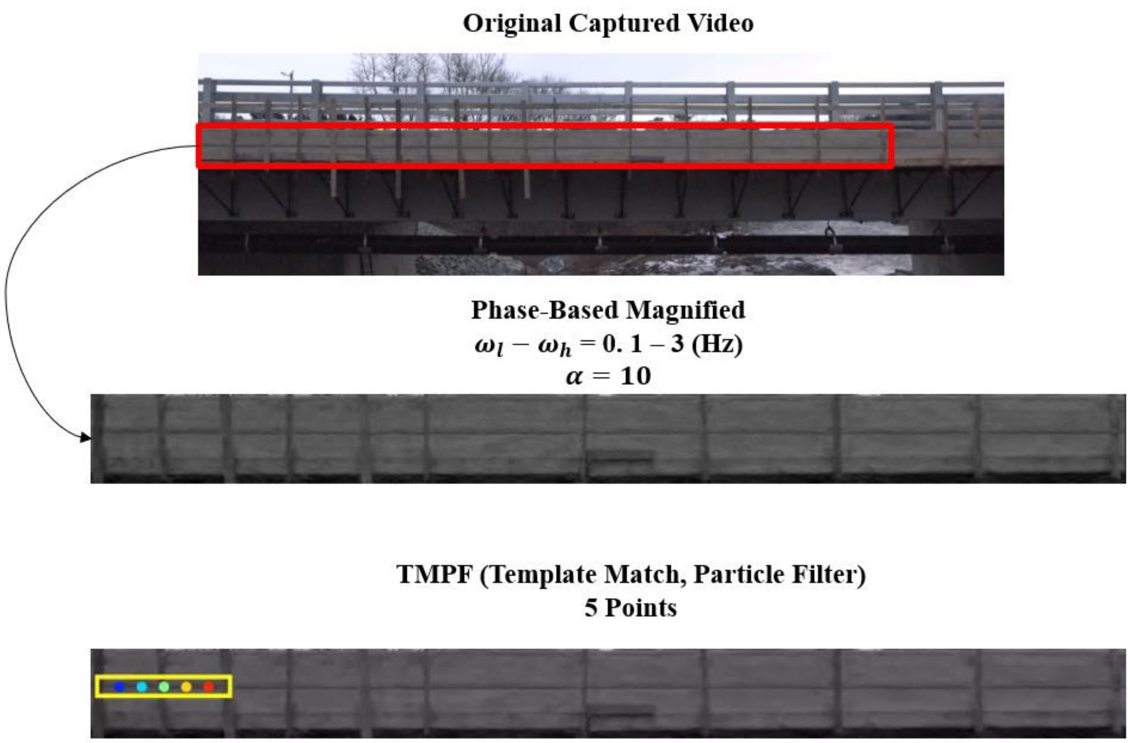

Fig. 5: Bridge data collection and magnification for frequency validation via TMPF.

A SONY PXW-FX9 XDCAM Full-Frame camera system at 60 (fps) was used to capture the raw video of the bridge. A calibration factor of 12 (mm/pixel) is computed utilizing the working distance of the camera. Fig. 6 displays the magnified time history and frequency for each RGB coded target.

This is a preprint version. The published version is available at:
https://doi.org/10.1007/978-3-031-04098-6_5

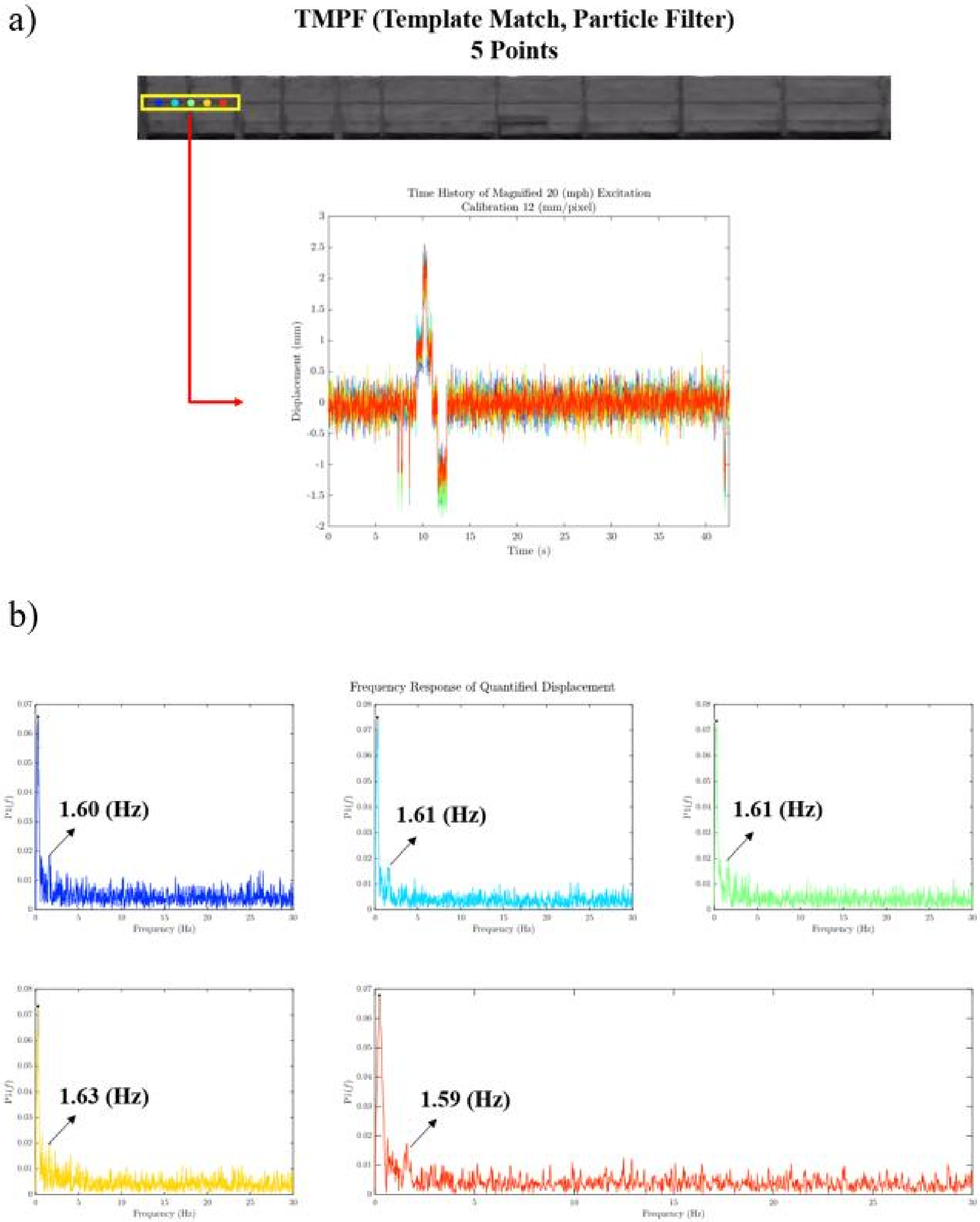

Fig. 6: (a) Magnified time history for a 20 (mph) excitation using five RGB coded targets, (b) Frequency response of magnified time history to identify the first resonant frequency.

Glancing at Fig. 6 (a), it is clear where the 20 (mph) excitation takes place during the captured video. TMPF can not only extract the dynamic motion at approximately 3 (mm), but it is also able to identify a resonant frequency of the bridge at approximately 1.6 (Hz).

This is a preprint version. The published version is available at:
https://doi.org/10.1007/978-3-031-04098-6_5

CONCLUSION

TMPF is a non-invasive computer vision approach that fuses a normalized cross-correlation between frames in addition to sub-pixel determination of magnified displacement. Hand speckle interferometry, commonly seen with techniques such as DIC, is an arduous pre-treatment of a particular region of interest. Also, the accuracy of said results are dependent on the size of each facet. TMPF serves to use the distinct features available in an image to make correlation between sequential frames. Particle filtering in conjunction with k-means clustering aid in gathering sub-pixel resolution of magnified displacement without having to pre-treat the structure. In addition to magnified time history, TMPF can also compute structural dynamic parameters such as resonant frequencies and operating deflection shapes. To further confirm the technique, a full-scale bridge structure was excited and its first resonant frequency was identified using the proposed algorithm. Future works will investigate the limitations of this approach, one major concerning being the rigidity of the template matching approach. At higher order dynamics, it becomes more cumbersome to place RGB coded targets if the region of interest contains two or more inflection points.

ACKNOWLEDGEMENTS

This material is based upon work supported by the National Science Foundation under Grant No. 1762809. Any opinions, findings, and conclusions or recommendations expressed in this material are those of the authors and do not necessarily reflect the views of the National Science Foundation. The authors would also like to acknowledge the support for the bridge testing provided by the Transportation Infrastructure Durability Center at the University of Maine under grant 69A3551847101 from the US Department of Transportation's University Transportation Centers Program.

REFERENCES

[1] N. Wadhwa, M. Rubinstein, F. Durand, and W. T. Freeman, "Phase-Based Video Motion Processing," *ACM Transactions on Graphics (TOG),* https://doi.org/10.1145/2461912.2461966 vol. 32, 2013.

[2] J. Chen, A. Davis, N. Wadhwa, F. Durand, W. T. Freeman, and O. Büyüköztürk, "Video Camera–Based Vibration Measurement for Civil Infrastructure Applications," *Journal of Infrastructure Systems,* https://doi.org/10.1061/(ASCE)IS.1943-555X.0000348 vol. 23, pp. B4016013-B4016013, 2016.

[3] C. T. do Cabo, N. A. Valente, and Z. Mao, "Motion magnification for optical-based structural health monitoring," in *Health Monitoring of Structural and Biological Systems XIV*, P. Fromme and Z. Su, Eds., 2020, vol. 11381: SPIE, pp. 221 – 227-221 – 227, doi: https://doi.org/10.1117/12.2559266.

[4] V. Fioriti, I. Roselli, A. Tatì, R. Romano, and G. De Canio, "Motion Magnification Analysis for Structural Monitoring of Ancient Constructions," *Measurement,* https://doi.org/10.1016/j.measurement.2018.07.055 vol. 129, 2018.

[5] Q. Li, G. Wang, A. Sarrafi, X. Niu, W. Lu, and Z. Mao, "Dynamic Characteristics Identification of an Arch Dam Model via the Phase-Based Video Processing," *KSCE Journal of Civil Engineering,* vol. 25, no. 1, pp. 140–152-140–152, 2021, doi: https://doi.org/10.1007/s12205-020-0400-z.

[6] A. Sarrafi, Z. Mao, C. Niezrecki, and P. Poozesh, "Vibration-based damage detection in wind turbine blades using Phase-based Motion Estimation and motion magnification," *Journal of Sound and Vibration,* vol. 421, pp. 300-318, 2018, doi: https://doi.org/10.1016/j.jsv.2018.01.050.

[7] N. A. Valente, Z. Mao, M. Southwick, and C. Niezrecki, "Implementation of Total Variation Applied to Motion Magnification for Structural Dynamic Identification," Cham, 2020: Springer International Publishing, in Rotating Machinery, Optical Methods & Scanning LDV Methods, Volume 6, pp. 139-144, doi: https://doi.org/10.1007/978-3-030-47721-9_17.

[8] C. Shi and G. Luo, "A Streaming Motion Magnification Core for Smart Image Sensors," *IEEE Transactions on Circuits and Systems II: Express Briefs,* https://doi.org/10.1109/TCSII.2017.2775583 vol. PP, pp. 1-1, 2017.

[9] Y. Bao, P. Seshadri, and S. Mahadevan, "Motion magnification for mode shape determination," in *58th AIAA/ASCE/AHS/ASC Structures, Structural Dynamics, and Materials Conference, 2017*, 2017.

[10] H. Hassoun, J. Hallal, D. Duhamel, M. Hammoud, and A. H. Diab, "Modal Analysis of a Cantilever Beam Using an Inexpensive Smartphone Camera: Motion Magnification Technique," *International Journal of Mechanical and Mechatronics Engineering,* vol. 15, no. 1, pp. 52-56, 2021. [Online]. Available: https://publications.waset.org/vol/169.

[11] J. Javh, J. Slavič, and M. Boltežar, "The subpixel resolution of optical-flow-based modal analysis," *Mechanical Systems and Signal Processing,* https://doi.org/10.1016/j.ymssp.2016.11.009 vol. 88, pp. 89-99, 2017.

[12] A. J. Molina-Viedma, L. Felipe-Sesé, E. López-Alba, and F. A. Díaz, "3D mode shapes characterisation using phase-based motion magnification in large structures using stereoscopic DIC," *Mechanical Systems and Signal Processing,* https://doi.org/10.1016/j.ymssp.2018.02.006 vol. 108, pp. 140-155, 2018.

[13] P. Poozesh, A. Sarrafi, Z. Mao, P. Avitabile, and C. Niezrecki, "Feasibility of extracting operating shapes using phase-based motion magnification technique and stereo-photogrammetry," *Journal of Sound and Vibration,* https://doi.org/10.1016/j.jsv.2017.06.003 2017.

[14] M. P. Popek, M. E. Danielewska, and D. R. Iskander, "Assessing frequency response of video motion magnification techniques," in *2017 Signal Processing Symposium (SPSympo)*, 2017/sep., pp. 1-4.

[15] D. P. Rohe and P. L. Reu, "Experimental Modal Analysis Using Phase Quantities from Phase-Based Motion Processing and Motion Magnification," *Experimental Techniques,* 2020, doi: https://doi.org/10.1007/s40799-020-00392-7.

[16] Z. Shang and Z. Shen, "Multi-point vibration measurement and mode magnification of civil structures using video-based motion processing," *Automation in Construction,* vol. 93, pp. 231-240, 2018, doi: https://doi.org/10.1016/j.autcon.2018.05.025.

[17] S. Aral and M. Zhu, "Structural operating deflection shape estimation via a hybrid computer-vision algorithm," in *Proc.SPIE*, 2018, vol. 10600, doi: https://doi.org/10.1117/12.2296784.

[18] K. Okuma, A. Taleghani, N. De Freitas, J. J. Little, and D. G. Lowe, "A boosted particle filter: Multitarget detection and tracking," in *European conference on computer vision*, 2004: Springer, pp. 28-39.

[19] J. N. Sarvaiya, S. Patnaik, and S. Bombaywala, "Image registration by template matching using normalized cross-correlation," in *2009 international conference on advances in computing, control, and telecommunication technologies*, 2009: IEEE, pp. 819-822.

[20] Z. Y. Wu, H. W. Shenton Iii, D. Mo, and M. Hmosze, "Integrated Video Analysis Framework for Vision-Based Comparison Study on Structural Displacement and Tilt Measurements," *Journal of Structural Engineering,* https://doi.org/10.1061/(ASCE)ST.1943-541X.0003104 vol. 147, no. 9, pp. 05021005-05021005, 2021.

[21] F. Cheli, P. Mazzoleni, M. Pezzola, E. Ruspini, and E. Zappa, "Vision-based measuring system for rider's pose estimation during motorcycle riding," *Mechanical Systems and Signal Processing,* vol. 38, no. 2, pp. 399-410, 2013/07/20/ 2013, doi: https://doi.org/10.1016/j.ymssp.2013.01.009.

[22] K. P. Sinaga and M. Yang, "Unsupervised K-Means Clustering Algorithm," *IEEE Access,* vol. 8, pp. 80716-80727, 2020, doi: 10.1109/ACCESS.2020.2988796.